PHYSICAL REVIEW C **71**, 051604(R) (2005)

Possibility to study a two-proton halo in ^{17}Ne

L. V. Grigorenko,[1] Yu. L. Parfenova,[2] and M. V. Zhukov[3]
[1]*Flerov Laboratory of Nuclear Reactions, JINR, RU-141980 Dubna, Russia*
[2]*Sholohov st., 7, 318, RU-119634, Moscow, Russia*
[3]*Fundamental Physics, Chalmers University of Technology, S-41296 Göteborg, Sweden*
(Received 15 October 2004; published 26 May 2005)

The nuclide ^{17}Ne is studied theoretically in a three-body ^{15}O+p+p model. We demonstrate that the experimental condition for existence of a proton halo in ^{17}Ne can be reasonably quantified in terms of s/d configuration mixing. We discuss experimental evidence for a proton halo in ^{17}Ne and define which kind of experimental data could elucidate this issue.

DOI: 10.1103/PhysRevC.71.051604 PACS number(s): 21.60.Gx, 21.10.Sf, 25.60.Dz, 25.60.Gc

The ^{17}Ne nucleus is an interesting but relatively poorly studied system. It is a Borromean nucleus, since none of the binary subsystems (^{15}O-p and p-p) are bound. It seems to be the only realistic candidate to possess a two-proton halo [1,2]. The level scheme was established not long ago [3] in multineutron transfer reactions. Available experimental data include Coulomb excitation [4,5] and low energy nuclear fragmentation [6,7] measurements. The ^{17}Ne nucleus has attracted attention also because of the possibility of two-proton emission from the excited states [2,4]. Another interesting issue related to mirror nucleus ^{17}N is a β-decay asymmetry for decays to the first excited $1/2^+$ states in daughter nuclei [8].

The results of theoretical studies of ^{17}Ne are controversial. Papers [2,9,10] studied the structure of ^{17}Ne with emphasis on the Coulomb displacement energy (CDE) derivation. In papers [9,11,12], the s^2 configuration was predicted to dominate, while in paper [10] the dominating configuration was predicted to be d^2. In paper [11], effects of the "halo" kind [connected with larger radial extension of wave function (WF) on the proton-rich side of the isobar] were considered irrelevant for the β-decay asymmetry problem [8]. However, paper [13] successfully explained the β-decay asymmetry in these terms. It seems that theoretical agreement about the basic properties of ^{17}Ne is still missing at the moment.

In papers [7,14], the comparatively narrow core momentum distribution was interpreted as possible evidence of a proton halo in ^{17}Ne. This is a reasonable approach to the problem, as among typical experimental evidence of the halo (e.g., large interaction, electromagnetic dissociation, and nucleon removal cross sections), the momentum distributions should give the most expressed signal for this system. The aim of this paper is to test three-body WFs, obtained in [2], against the most recent experimental data [5,7]. We demonstrate that the experimental question of the proton halo existence in ^{17}Ne formulated as in [7,14] is largely defined by s/d configuration mixing. As we have already mentioned, the exact s/d ratio in ^{17}Ne is difficult to obtain unambiguously by theoretical calculations. To derive it from experimental data, it is necessary to know the sensitivity of various observables to this aspect of the dynamics. We show that currently available experimental data are insufficient to determine reliably the structure (and possible halo properties) of ^{17}Ne. We can, however, confidently define which kind of experimental data is required to resolve the puzzling issues of the ^{17}Ne structure.

Structure model. Studies in this paper are based on the ^{17}Ne WF obtained in a three-body model [2]. The model predicts about 50% s/d mixing for the ground state of ^{17}Ne. Recently this nucleus has been studied in a three-body model [15], providing results very close to those in Ref. [2]. Besides the WF from [2], which we refer to here as GMZ, we have also generated two WFs with high [$W(s^2) \sim 70\%$] and low [$W(s^2) \sim 7\%$] weights of s^2 components. Note that this required unrealistic modifications of the ^{16}F spectra. Thus, these WFs should not be regarded as variants of a theoretical prediction. They are used in this paper only to estimate a scale of the sensitivity of different observables to variations in ^{17}Ne structure. Table I and Fig. 1 show various properties of the three lowest states in ^{17}N and ^{17}Ne calculated with realistic GMZ, "high s," and "low s" WFs.

Studies of the ^{17}N-^{17}Ne pair as core+N+N systems are reasonably well motivated. The nuclei ^{15}N and ^{15}O are well suited for the role of cores in a cluster model. Their lowest excitations are located at about 5.2 MeV, and the lowest particle decay thresholds are at 10.2 and 7.3 MeV, respectively. Also, in shell model studies of ^{17}N [16] and ^{17}Ne [13] the admixture of excited core configurations was found to be below 5%, which is not enough to significantly change "bulk" properties of these nuclei. The core matter radius enters the definition of the composite system radius, the core charge radius is used to define a Coulomb interaction (if needed). For ^{15}N the charge radius is known from electron scattering $r_{\rm ch}(^{15}{\rm N}) = 2.615$ fm [17]. The corresponding matter radius is $r_{\rm mat}(^{15}{\rm N}) = 2.49$ fm. We estimated the matter radius of ^{15}O in two ways [from known experimental charge radii $r_{\rm ch}(^{14}{\rm N}) = 2.57$ fm and $r_{\rm ch}(^{16}{\rm O}) = 2.71$ fm], providing the same result: $r_{\rm mat}(^{15}{\rm O}) = 2.53$ fm.

CDE. This is the only observable for which a sensitivity to ^{17}Ne structure far exceeds an experimental uncertainty. Calculations [2] provide the WF with about 50% s/d mixing (GMZ case) reproducing experimental CDE very well. We rely much on this fact, as a correct CDE guarantees very reasonable radial characteristics of the WF. However, there is

TABLE I. Structure and observables for ^{17}N and ^{17}Ne. The experimental CDE for ^{17}N-^{17}Ne isobaric pair is $\Delta E_c(1/2^-) = 7.430$ MeV. Properties of ground $1/2^-$ states are given in the first six rows. Properties of excited $3/2^-$ and $5/2^-$ states are given in the last six rows. The $B(E2)$ values are given in e^2 fm^4. For ^{17}N they are calculated with the rigid core; those for ^{17}Ne are corrected for experimental $B(E2)$ of ^{17}N. $W(i)$ are weights of dominating WF configurations in percent.

Nucleus:	^{17}N			^{17}Ne		
WF:	"low s"	GMZ	"high s"	"low s"	GMZ	"high s"
$W(s^2)$	7.3	39.8	63.4	4.8	48.1	73.4
$W(p^2)$	2.2	4.5	3.2	1.0	4.0	2.5
$W(d^2)$	90.4	55.6	33.0	94.0	47.8	23.8
r_{mat} (fm)	2.59	2.61	2.63	2.65	2.69	2.73
$\langle\rho\rangle$ (fm)	4.59	4.81	5.00	4.82	5.22	5.49
ΔE_c (MeV)				7.685	7.424	7.194
$W(sd, 3/2)$	50.9	72.9	93.8	56.3	76.1	94.8
$W(d^2, 3/2)$	46.6	24.0	4.5	41.1	20.9	3.6
$B(E2, 3/2)$	0.01	0.18	0.11	17.1	59.4	40.3
$W(sd, 5/2)$	7.6	69.8	41.4	9.2	73.0	57.9
$W(d^2, 5/2)$	91.4	27.0	58.3	89.7	23.9	41.7
$B(E2, 5/2)$	0.00	0.29	0.00	16.8	94.7	12.3

no agreement among theorists on this issue, and other checks are also necessary.

E2 transitions. Experimental derivation of $B(E2)$ values for the first excited states of ^{17}Ne is a significant advance in studies of this system: $B(E2, 1/2 \to 3/2) = 66^{+18}_{-25}\ e^2$ fm^4 [4] and $B(E2, 1/2 \to 5/2) = 124(18)\ e^2$ fm^4 [5]. If we consider the ^{15}O core as a rigid charged body, its contribution to $B(E2)$ of ^{17}Ne in a three-body model is small because of the large core mass. The $B(E2)$ values are underestimated by 30–50% in such calculations. To improve the model, we extract the $E2$ matrix element $M(E2)_{\mathrm{core}}$ for the core from the experimental value $B(E2, 1/2 \to 5/2) = 6.7(1.2)\ e^2$ fm^4 for ^{17}N [18]. It is possible to do this because here valence neutrons do not contribute the $B(E2)$ value. The resulting calculated $B(E2)$ values for different versions of ^{17}Ne WFs are given in Table I (see also Fig. 1). One can see that only in the case of a significant configuration mixing can good agreement with experimental values be achieved.

Large, compared to ours, theoretical $B(E2)$ values were obtained in shell model calculations with effective charges [5]: 105 and 155 e^2 fm^4 for transitions to $3/2^-$ and $5/2^-$ states. Note that in our calculations there are no effective charges. If we recalculate our $B(E2)$ values using effective charges from [5], we get good agreement with these calculations for GMZ WF.

Momentum distributions. The first step in studies of momentum distributions from fragmentation reactions is to study the momentum distribution in the nucleus itself. Figure 2 shows momentum distributions of particles from the valence part of the ^{17}Ne WF. One can see that in momentum space, ^{17}Ne WFs have two distinctive components, connected with s^2 and d^2 configurations. Depending on the ratio of these components, momentum distributions for ^{17}Ne could be either broader or narrower than the corresponding distributions for the ^{6}He halo nucleus. For realistic GMZ WF, the momentum distributions seem to be relatively close to that for ^{6}He with average momenta being approximately the same.

The internal momentum distributions can be related to the proton sudden removal approximation for high energy reactions. If the final state interaction (FSI) of the ^{15}O core with a proton can be neglected, then measured core momentum distributions are simply the core momentum distributions in ^{17}Ne [Fig. 2(a)]. Corresponding longitudinal momentum distributions (LMDs) of the core are shown in Fig. 3(a). Both WFs with large s^2 weights give core LMDs as narrow as the core LMD in ^{6}He. Only the core distribution for "low s" WF has a larger full width at half maximum (FWHM) of 184 MeV/c.

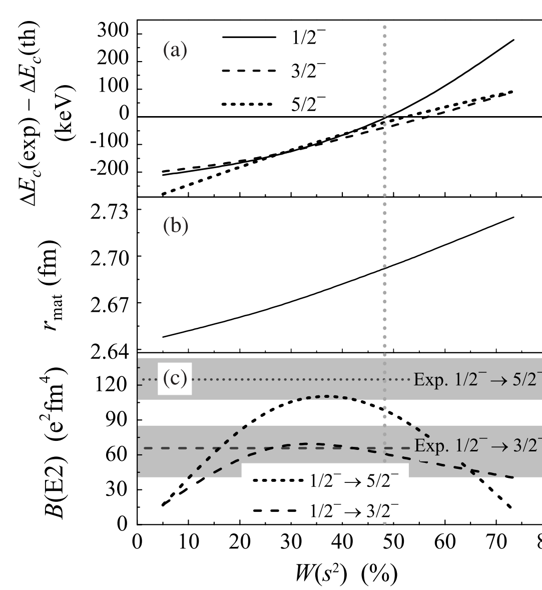

FIG. 1. Dependence of observables for ^{17}Ne on the structure. (a) Difference of experimental and theoretical CDEs for ^{17}N-^{17}Ne pair. (b) Matter radius. (c) $B(E2)$ probabilities for transitions between ground state and first excited states. The vertical dotted line corresponds to $W(s^2)$ of the GMZ WF.

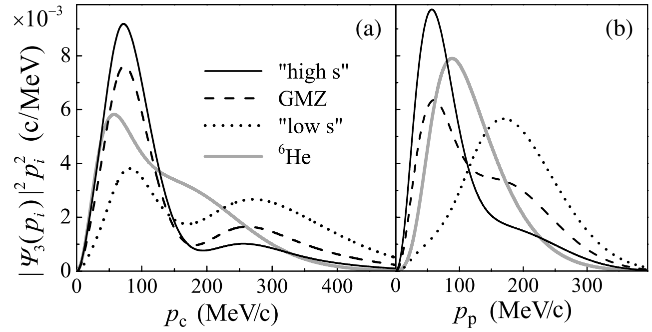

FIG. 2. Momentum distributions of a core (a) and a valence nucleon (b) in ^{6}He WF and in different ^{17}Ne WFs.

The inclusion of the FSI between the core and a proton can also lead to more narrow distributions [19,20]. Taking into account resonance states in the ^{16}F subsystem formed after knockout of a valence proton, the core LMD can be considered as [20]

$$\frac{dN}{dp_{c\parallel}} \sim \sum_M \int d^3p_x\, d^3p_y\, d^2p_{c\perp}\, \delta\big(\tfrac{15}{16}\mathbf{p}_y + \mathbf{p}_x - \mathbf{p}_c\big) \times \sum_\sigma \left|\sum_{jm}\langle \Psi_3^{JM}(\mathbf{X},\mathbf{Y}) \,|\, \Psi_2^{jm}(\mathbf{p}_x,\mathbf{X}) e^{i\mathbf{p}_y\mathbf{Y}}\chi_p\rangle\right|^2, \quad (1)$$

where $\Psi_2^{jm}(\mathbf{p}_x, \mathbf{X})$ are the WFs of ^{16}F resonance states with different j^π, χ_p is a spin function of a removed proton, and σ stands for summation over spin variables. The Jacobi coordinates $\mathbf{X}, \mathbf{Y}$ and the conjugated momenta $\mathbf{p}_x, \mathbf{p}_y$ are in the "Y" coordinate system ($\mathbf{X}$ is a distance between the core and a valence proton). This mechanism is dominating, e.g., in fragmentation of ^{6}He and ^{11}Li [21]. Four low-lying single-particle states in ^{16}F are taken into account: 0^-, 1^-, 2^-, and 3^- with energies 0.535, 0.728, 0.959, and 1.256 MeV above the ^{15}O$+p$ threshold. The calculated distributions (1), shown in Fig. 3(b), agree well with the "no FSI" approximation Fig. 3(a) for "high s" and GMZ WFs. In the "low s" case the shapes of the distributions are different (due to strong correlations in the d^2 WF), but the rms longitudinal momenta $\langle p_{c\parallel}^2\rangle^{1/2}$ for these distributions are reasonably close (they are 150 and 113 MeV/c for Figs. 3(a) and 3(b), respectively). It

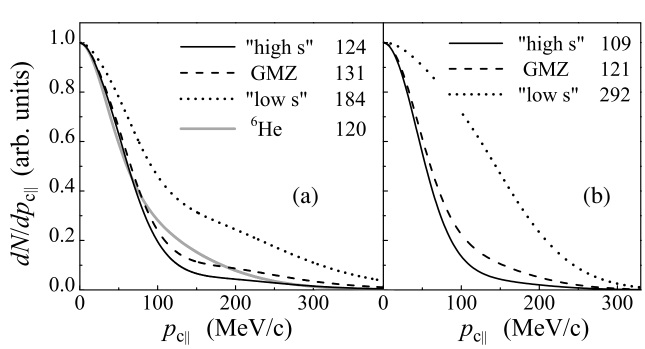

FIG. 3. Longitudinal core momentum distributions for ^{6}He WF and for different ^{17}Ne WFs. (a) "No FSI" approximation. (b) Population of four low-lying resonances in ^{16}F. The values in the legends are FWHM of distributions in MeV/c.

TABLE II. Experimental [6] and theoretical interaction cross sections σ_I (in mb) for the ^{15}O$+^{28}$Si reaction.

$E_{\rm beam}$ (MeV/nucleon)	22.0–30.8	30.8–38.0	38.0–44.0
σ_I(exp)	1740(40)	1790(40)	1680(40)
σ_I(th)	1860	1780	1725

is known [22,23] that the core "shadowing" effect will lead to realistic momentum distributions which are only narrower than those obtained in the sudden removal approximation. Thus, looking at these figures one could conclude that experimental data [7] giving FWHM 168(17) MeV/c for LMD of the ^{15}O core support the case of d^2 domination in the structure of ^{17}Ne [$W(s^2) < 25\%$]. There is, however, an obstacle which makes the analysis of the situation more complicated.

Interaction cross sections. Interaction and proton removal cross sections are calculated in the eikonal approximation of the Glauber model [24] for three-body ^{17}Ne nucleus. In this model, breakup cross sections are related to interaction cross sections of the fragments as

$$\sigma_{\rm str}^{1p} + \sigma_{\rm str}^{2p} + \sigma_{\rm dif} = \sigma_{-2p} = \sigma_I(^{17}{\rm Ne}) - \sigma_I(^{15}{\rm O}). \quad (2)$$

In our calculations the cross sections are determined by the interaction potential [23] generated from the free NN interaction [25] and nuclear fragment densities.

The ^{9}Be density ρ is parametrized by the modified harmonic oscillator expression [26] with $a = 1.791$ fm $\rho(r) = \rho_0[1 + \alpha(r/a)^2]\exp[-(r/a)^2]$, which gives the ^{9}Be charge radius 2.52 fm. The ^{12}C and ^{28}Si densities are approximated by the sum of Gaussians with parameters from Ref. [26]. The ^{15}O density distribution is not known; we approximate it by the two-parameter Fermi expression $\rho(r) = \rho_0/\{1 + \exp[(r - c)/z]\}$ [26]. Parameters $c = 3.266$ fm and $z = 0.1$ fm are chosen to reproduce both the ^{15}O matter radius and interaction cross sections for reactions ^{15}O$+^{28}$Si at energies 22–44 MeV/nucleon [6] (Table II) and ^{15}O$+^{9}$Be, ^{15}O$+^{12}$C at the energy 710 MeV/nucleon [27] (Table III).

This choice of core and target densities allows us to reproduce the experimental data on the $p+^{28}$Si [28] and ^{17}Ne$+^{28}$Si [6] interaction cross sections at 20–50 MeV/nucleon [6] (Table IV). The agreement with experiment for the p, ^{15}O, and ^{17}Ne interaction cross sections on ^{9}Be and ^{12}C targets is also very good for two available experimental energies (Table III). All results for ^{17}Ne in Tables III and IV are calculated with the GMZ WF. The matter radius for our WF (Table I) is also in agreement with the effective $r_{\rm mat}^{\rm exp} = 2.75(7)$ fm extracted in the Glauber model with harmonic-oscillator densities [29].

Proton removal from halo in ^{17}Ne. Contrary to the total interaction cross sections, the $2p$ removal cross sections are 30–40% underestimated in our calculations (see Tables III and IV). To check the sensitivity of the cross sections to variations of the ^{17}Ne structure, we calculated the $2p$ removal cross sections for ^{17}Ne on Be target at 66 MeV/nucleon with different ^{17}Ne WFs. The corresponding σ_{-2p} are 120, 109, and 82 mb for "high s," GMZ, and "low s" WFs. These results show that this variation of the ^{17}Ne structure is not sufficient to compensate for the discrepancy with experiment.

TABLE III. Experimental and theoretical cross sections (in mb) for p,^{15}O, and ^{17}Ne on different targets at 710 and 66 MeV/nucleon. The experimental values for ^{17}Ne from [27], measured at the energy 680 MeV/nucleon, are scaled according to the energy dependence of the interaction cross section.

Target	$\sigma_I(p)$	$\sigma_I(^{15}\text{O})$	$\sigma_I(^{17}\text{Ne})$	$\sigma_{-2p}(^{17}\text{Ne})$
	$E_{\text{beam}} = 710$ MeV/nucleon			
Be(exp)	214(13) [28]	912(23) [27]	972(45) [27]	
Be(th)	210	914	987	73
C(exp)	232(14) [28]	922(49) [27]	1094(76) [27]	
C(th)	240	970	1050	80
	$E_{\text{beam}} = 66$ MeV/nucleon			
Be(exp)	316 [28]			191(48) [7]
Be(th)	308	1070	1179	109

To overcome this problem, it was suggested in Ref. [7] that (i) the halo is very large ($\langle r_p \rangle \sim 4.5$ and 3.8 fm for pure s^2 and d^2 configurations compared to $\langle r_p \rangle \sim 3.7$, 3.5, and 3.3 fm given by "high s," GMZ, and "low s" WFs) and (ii) the matter radius of the ^{15}O core is small ($r_{\text{mat}} = 2.42$ fm compared to 2.53 fm in this work). Only these (too strong, in our opinion) assumptions provided $\sigma_{-2p}(\text{th}) \sim 168$ mb [7] for the pure s^2 configuration in an agreement with experiment. In our model, the halo size is fixed by the CDE, and a reduction of the core size leads to a deterioration of the agreement for multiple calculated reaction cross sections. We do not feel there is freedom in that direction and that other explanations are required.

The calculated σ_{-2p} values (see Table III) for 710 MeV/nucleon on the C target of about 40 mb "per proton" are in qualitative agreement with the theoretical proton knockout cross sections from ^{8}B (about 80 mb [30]), which are also in good agreement with experimental data. It is expected that in ^{8}B the halo feature is more expressed than in ^{17}Ne because of the smaller Coulomb interaction and smaller binding energy. Also, the ^{7}Be core in ^{8}B is smaller than the ^{15}O core in ^{17}Ne, increasing the probability of the ^{7}Be core survival. Otherwise, if we explain the whole two-proton removal cross section in ^{17}Ne [7] as a removal from the halo we come to a contradiction. From this cross section, it should then be concluded that in ^{17}Ne the halo is much more pronounced than in ^{8}B (which is not in accord with general expectations), whereas from momentum distribution [7] (which is relatively broad) a pronounced halo in ^{17}Ne should not be expected.

Proton removal from the ^{15}O *core*. The possible solution of the above problem could be to incorporate processes that are beyond a simple valence nucleon removal. For the case of ^{11}Be (one neutron halo nucleus), papers [31–33] showed that besides the valence nucleon removal, the removal of a tightly bound core nucleon leading to low-lying excited states of a fragment can also give an important contribution to the cross section. For the ^{17}Ne case, it means that a process of p-wave proton removal from ^{15}O core has to be considered (see also [7], "model-3"). The simplest possible mechanism is schematically illustrated in Fig. 4. A p-wave proton knockout from the ^{15}O $(1/2^-)$ core leads to ^{14}N in 1^+ states. These states together with the valence protons (which are predominantly in the 0^+ relative motion state in ^{17}Ne) could populate 1^+ states in ^{16}F located below the ^{14}N+$2p$ threshold. These states decay only via the ^{15}O+p channel and thus contribute the two-proton removal cross section for ^{17}Ne.

The calculated cross section of the $p_{1/2}$ proton removal from the ^{15}O nucleus with the proton separation energy $S_p = 7.279$ MeV is $\sigma_{-p} = 19.4$ mb, and the FWHM of the LMD is 177 MeV/c. The removal cross section of the $p_{3/2}$ proton with $S_p = 11.247$ MeV is $\sigma_{-p} = 15.3$ mb and FWHM = 200 MeV/c. Taking into account two protons in the $p_{1/2}$ state and four protons in the $p_{3/2}$ state, we get an assessment of the proton removal cross section of 100 mb and FWHM = 190 MeV/c, which is in good agreement with the experimental data 80(10) mb and 190(10) MeV/c from [14] for the beam energy 56 MeV/nucleon. The cross section of the proton removal from the ^{15}O core is obtained in the three-body model similarly to [33]: $\sigma_{-p} = 53$ mb. Together with the $2p$ removal from the halo this provides the total $2p$ removal cross section of 162 mb, which agrees with the results from [7]. Thus, the broad momentum distribution [168(17) MeV/c] found in [7] cannot be proof of d^2 domination in the ^{17}Ne halo as these

TABLE IV. Experimental [6] and theoretical interaction and $2p$ removal cross sections (in mb) for the ^{17}Ne+^{28}Si reaction.

E_{beam} (MeV/nucleon)	σ_I(exp)	σ_{-2p}(exp)	σ_I (th)	σ_{-2p} (th)
27.6–37.7	1980(70)		1950	155
37.7–46.3	1930(70)		1868	149
46.3–53.3	1770(70)		1813	145
46		260(30)		147

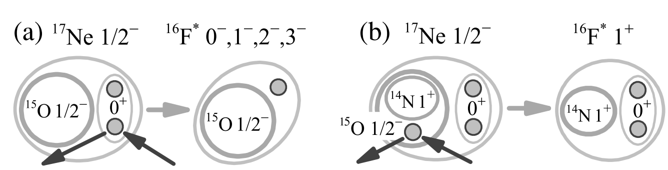

FIG. 4. Dominating reaction mechanisms for one-proton knockout from ^{17}Ne. (a) s/d-wave proton knockout from halo, populating negative parity states in ^{16}F. (b) p-wave proton knockout from ^{15}O core, populating 1^+ states in ^{16}F.

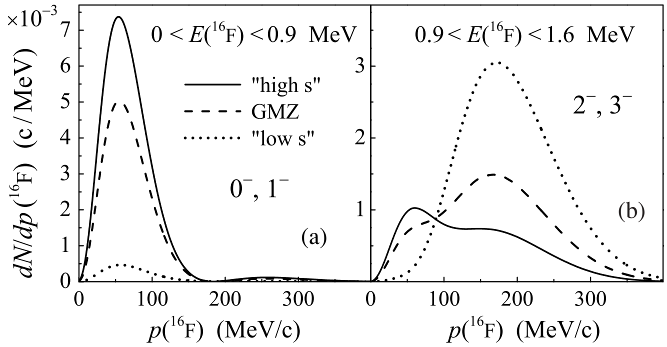

FIG. 5. Momentum distribution of ^{16}F c.m. for proton knockout from ^{17}Ne gated on the energy ranges with *š*-wave (a) and *d*-wave (b) negative parity states in ^{16}F.

data are presumably strongly influenced by the processes on the core.

Invariant mass measurement of ^{16}F. It is easy to disentangle halo and core contributions to the two-proton removal cross section in an exclusive experiment. The invariant mass measurement of ^{15}O and proton should allow us to distinguish the processes of proton knock out from the halo (which should mainly proceed through low-lying negative parity states in ^{16}F) and proton knock out from the core (which involves 1^+ states of ^{16}F). From spectroscopic considerations, the populations of the energy ranges for relative motion of p and ^{15}O corresponding to $0^-, 1^-, 2^-$, and 3^- states in ^{16}F are proportional to $\frac{1}{4}W(s^2)$, $\frac{3}{4}W(s^2)$, $\frac{1}{4}W(d^2)$, and $\frac{7}{20}W(d^2)$ in the first approximation. The real situation could be more complicated, and exclusive momentum distributions can help to improve the understanding. The momentum distributions of ^{16}F c.m. calculated in the same model as Eq. (1) and gated on different ranges of excitation energy in ^{16}F (where there are only negative parity states) are shown in Fig. 5. If the reaction mechanism of the model Eq. (1) prevails, such experimental distributions should be free from the core contributions. Moreover, the ratios and shapes of the corresponding distributions in Figs. 5(a) and 5(b) are strongly sensitive to the structure of the halo in ^{17}Ne. So, comparison of such distributions could make it possible to obtain conclusive information on this issue.

Conclusion. The question of the existence of a proton halo in ^{17}Ne, approached from the experimental side, can be quantified as the question of s/d configuration mixing. In the case of a significant (say, $\geqslant 50\%$) s-wave component in the ^{17}Ne WF, the "classical" fingerprints of the halo should exist, e.g., narrow core momentum distributions for valence proton knock out. These distributions should have comparable widths to the corresponding distributions in the ^{6}He case, which is a recognized example of a halo nucleus. There is considerable experimental evidence [CDE, B(E2)] that the halo part of ^{17}Ne WF is a significant mixture of s^2 and d^2 configurations.

The proton removal from the halo is likely to be responsible only for 60–70% of the two-proton removal cross section from ^{17}Ne. The rest is possibly connected with the proton removal from the core. Thus, consideration of inclusive LMD of the core is insufficient to draw conclusions about the halo property of ^{17}Ne, as this characteristic can have a large contribution from processes on the core. The question about configuration mixing in ^{17}Ne can be resolved by invariant mass measurement of ^{15}O and a spectator proton after proton knockout.

The authors acknowledge the financial support from the Royal Swedish Academy of Science, Russian RFBR Grant 02-02-16174, and Russian Ministry of Industry and Science Grant NS-1885.2003.2.

[1] M. V. Zhukov and I. J. Thompson, Phys. Rev. C **52**, 3505 (1995).
[2] L. V. Grigorenko, I. G. Mukha, and M. V. Zhukov, Nucl. Phys. **A713**, 372 (2003); **A740**, 401(E) (2004).
[3] V. Guimarães *et al.*, Phys. Rev. C **58**, 116 (1998).
[4] M. J. Chromik *et al.*, Phys. Rev. C **55**, 1676 (1997).
[5] M. J. Chromik *et al.*, Phys. Rev. C **66**, 024313 (2002).
[6] R. E. Warner *et al.*, Nucl. Phys. **A635**, 292 (1998).
[7] R. Kanungo *et al.*, Phys. Lett. **B571**, 21 (2003); R. Kanungo, Nucl. Phys. **A738**, 293 (2004).
[8] M. J. G. Borge *et al.*, Phys. Lett. **B317**, 25 (1993).
[9] S. Nakamura, V. Guimarães, and S. Kubono, Phys. Lett. **B416**, 1 (1998).
[10] H. T. Fortune and R. Sherr, Phys. Lett. **B503**, 70 (2001).
[11] N. K. Timofeyuk, P. Descouvemont, and D. Baye, Nucl. Phys. **A600**, 1 (1996).
[12] R. K. Gupta *et al.*, J. Phys. G **28**, 699 (2002).
[13] D. J. Millener, Phys. Rev. C **55**, R1633 (1997).
[14] H. Jeppesen *et al.*, Nucl. Phys. **A739**, 57 (2004).
[15] E. Garrido, D. V. Fedorov, and A. S. Jensen, Phys. Rev. C **69**, 024002 (2004); Nucl. Phys. **A733**, 85 (2004).
[16] H. Ueno *et al.*, Phys. Rev. C **53**, 2142 (1996).
[17] F. Ajzenberg-Selove, Nucl. Phys. **A523**, 1 (1991).
[18] D. R. Tilley and H. R. Weller, Nucl. Phys. **A564**, 1 (1993).
[19] A. A. Korsheninnikov *et al.*, Europhys. Lett. **29**, 359 (1995); T. Nilsson *et al.*, Nucl. Phys. **A598**, 418 (1996).
[20] E. Garrido, D. V. Fedorov, and A. S. Jensen, Phys. Rev. C **53**, 3159 (1996).
[21] T. Aumann, L. V. Chulkov, V. N. Pribora, and M. H. Smedberg, Nucl. Phys. **A640**, 24 (1998).
[22] P. G. Hansen, Phys. Rev. Lett. **77**, 1016 (1996).
[23] K. Hencken, G. Bertsch, and H. Esbensen, Phys. Rev. C **54**, 3043 (1996).
[24] G. F. Bertsch, K. Hencken, and H. Esbensen, Phys. Rev. C **57**, 1366 (1998).
[25] L. Ray, Phys. Rev. C **20**, 1857 (1979).
[26] H. DeVries, C. W. DeJager, and C. DeVries, At. Data Nucl. Data Tables **36**, 495 (1987).
[27] A. Ozawa, T. Suzuki, and I. Tanihata, Nucl. Phys. **A693**, 32 (2001).
[28] V. S. Barashenkov, in *Interaction Cross Sections of Particle and Nuclei with Nuclei* (JINR, Dubna, 1993) (in Russian).
[29] A. Ozawa *et al.*, Phys. Lett. **B334**, 18 (1994).
[30] Yu. L. Parfenova and M. V. Zhukov, Phys. Rev. C **66**, 064607 (2002).
[31] J. A. Tostevin, J. Phys. G **25**, 735 (1999).
[32] T. Aumann *et al.*, Phys. Rev. Lett. **84**, 35 (2000).
[33] Yu. L. Parfenova, M. V. Zhukov, and J. S. Vaagen, Phys. Rev. C **62**, 044602 (2000).